ACS Chemical Neuroscience

pubs.acs.org/chemneuro

Research Article

Validation of Dexamethasone-Enhanced Continuous-Online Microdialysis for Monitoring Glucose for 10 Days after Brain Injury

Emily K. Gifford, Elaine M. Robbins, Andrea Jaquins-Gerstl, Michael T. Rerick, Enyinna L. Nwachuku, Stephen G. Weber, Martyn G. Boutelle, David O. Okonkwo, Ava M. Puccio, and Adrian C. Michael*

Cite This: *ACS Chem. Neurosci.* 2021, 12, 3588–3597

Read Online

ACCESS | Metrics & More | Article Recommendations | Supporting Information

ABSTRACT: Traumatic brain injury (TBI) induces a pathophysiologic state that can be worsened by secondary injury. Monitoring brain metabolism with intracranial microdialysis can provide clinical insights to limit secondary injury in the days following TBI. Recent enhancements to microdialysis include the implementation of continuously operating electrochemical biosensors for monitoring the dialysate sample stream in real time and dexamethasone retrodialysis to mitigate the tissue response to probe insertion. Dexamethasone-enhanced continuous-online microdialysis (Dex-enhanced coMD) records long-lasting declines of glucose after controlled cortical impact in rats and TBI in patients. The present study employed retrodialysis and fluorescence microscopy to investigate the mechanism responsible for the decline of dialysate glucose after injury of the rat cortex. Findings confirm the long-term functionality of Dex-enhanced coMD for monitoring brain glucose after injury, demonstrate that intracranial glucose microdialysis is coupled to glucose utilization in the tissues surrounding the probes, and validate the conclusion that aberrant glucose utilization drives the postinjury glucose decline.

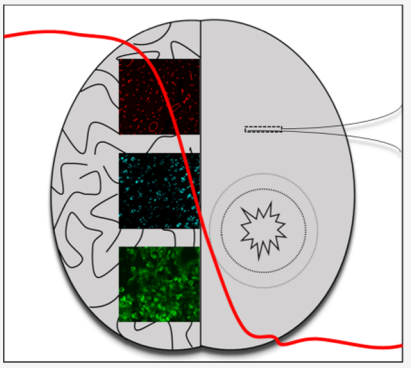

KEYWORDS: *microdialysis, dexamethasone, glucose, biosensor, traumatic brain injury, controlled cortical impact*

INTRODUCTION

Traumatic brain injury (TBI) has a global incidence of 69 million cases per year and represents a major public health crisis in many countries.[1] Causes of TBI include falls, vehicle accidents, sports injuries, military action, blasts, and assaults. Negative TBI outcomes can include long-lasting disabilities, a persistent vegetative state, and death.[2,3] The pathophysiology of severe TBI includes at-risk tissue or penumbra vulnerable to secondary injury, which can worsen the extent of injury.[4−6] We hypothesize that improved detection and monitoring of secondary injury will lead to more effective clinical care for TBI.

Intracranial microdialysis was first translated to the human brain by Ungerstedt and colleagues[7,8] and is approved for use in human patients.[9] Clinical microdialysis has established correlations between brain metabolite levels and outcomes for TBI patients,[10−14] which suggests that microdialysis has the potential to diagnose secondary injury. This potential motivates ongoing efforts to enhance microdialysis and its clinical utility, particularly in the intensive care setting.

Recent enhancements include the introduction of continuous-online microdialysis (coMD), in which the dialysate stream is analyzed with electrochemical biosensors mounted in a three-dimensional (3D)-printed holder.[15] The biosensors deliver information in real time, with sufficient temporal resolution to resolve chemical transients associated with spreading depolarization (SD).[5,16,17] coMD has a small physical footprint and operates autonomously for extended periods at the bedside: these features are highly desired in the intensive care setting.

Microdialysis is further enhanced by strategies to mitigate the foreign body response of brain tissues to probe insertion.[18,19] Without mitigation, probe insertion leads to focal ischemia, gliosis, and cell loss at the probe track,[20] which degrade the functionality of microdialysis.[21] Retrodialysis of low concentrations of dexamethasone (Dex), a powerful anti-inflammatory agent, is a simple yet effective mitigation strategy.[22−24]

Recently, we used Dex-enhanced microdialysis to monitor K^+ and glucose in the rat cortex for 10 days after controlled cortical impact (CCI),[25] a widely studied animal model of brain injury.[26−28] Consistent with other studies,[24,29,30] we observed both K^+ and glucose transients associated with SD. We also observed long-term changes in K^+ and glucose levels. In 80% of injured rats, glucose levels declined to levels too low to measure, possibly indicating the onset of metabolic abnormality after CCI. Herein, we further report that a

Received: April 12, 2021
Published: September 10, 2021

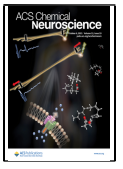

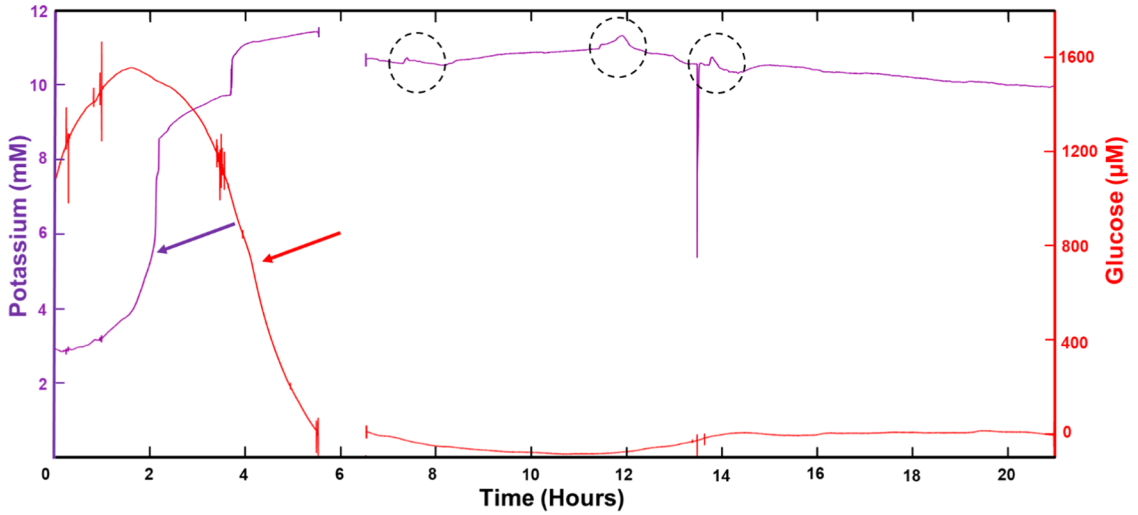

Figure 1. Sample recording of K^+ (purple) and glucose (red) obtained by bedside Dex-enhanced coMD in a patient 6 days after TBI. The recordings exhibit K^+ transients (circles), a long-term glucose decline (red arrow), and a long-term increase in K^+ (purple arrow). Monitoring was interrupted near hour 6 for system maintenance.

glucose decline has been observed during the first use of Dex-enhanced coMD in a small group of TBI patients.

The present study employed retrodialysis and fluorescence microscopy to investigate the mechanism responsible for the glucose decline after CCI. The findings confirm the long-term functionality of Dex-enhanced coMD for monitoring brain glucose after CCI, demonstrate that dialysate glucose levels are coupled to glucose utilization in the tissues surrounding the probes, and validate the conclusion that aberrant glucose utilization drives the glucose decline.

RESULTS AND DISCUSSION

Concordance between Dex-Enhanced Microdialysis after CCI and TBI. Recently, we used Dex-enhanced microdialysis to monitor K^+ and glucose from the rat cortex for 10 or more days after CCI.[25] There were four key outcomes: (1) K^+ transients indicative of SD, (2) glucose transients associated with some, but not all, K^+ transients, (3) long-term increases in K^+, and (4) long-term declines in glucose. The glucose decline, the main focus of the present study, was observed in 80% of injured rats, began between 2 and 11 days after CCI, followed various time courses, and was of sufficient magnitude that glucose levels fell to essentially zero, i.e., to below the detection limit of the glucose biosensor (20 μM; see the Methods section and Figure S1). After declining, glucose levels did not recover within the time frame of the experiments.

Figure 1 reports on our initial experience with monitoring K^+ and glucose with bedside Dex-enhanced coMD in a small group of patients (n = 4) with severe TBI following a motor vehicle accident (two patients), a bicycle accident (one patient), or a fall (one patient). The primary lesions in these patients were classified as subdural hemorrhage: on evaluation 6 months after injury, these patients scored from 1 to 5 on the Extended Glasgow Outcome Scale. It is important to note that there are several differences between the protocols for microdialysis in animals and patients. The probes are different, as are the procedures for probe placement. In animals, we surgically placed the probes adjacent to the CCI site. In patients, the probes were placed via a cranial bolt in the less affected frontal lobe in the hemisphere opposite the primary lesion. The location of the bolt was dictated by the clinical choice for the placement of intraparenchymal intracranial pressure (Camino Probe, Natus Medical, Pleasanton, CA) and brain oxygenation (Licox Probe, Integra Life Sciences, Princeton, NJ) probes based on CT imaging and in accordance with the site-specific standard of care.

Bedside Dex-enhanced coMD reproduced three of the four key outcomes of the CCI model (Figure 1): (1) K^+ transients (highlighted by circles), (2) a long-term increase in K^+, and (3) a long-term decline in glucose to essentially zero (to date, we have not observed glucose transients accompanying K^+ transients). The representative recordings in Figure 1 were obtained 6 days after probe insertion. Prior to the 6th day, the K^+ and glucose levels had been steady and unremarkable. The recordings in Figure 1 include a 1 h break, during which regularly scheduled system maintenance, including removal, calibration, and replacement of the coMD biosensors, was performed. The K^+ and glucose levels were similar before and after system maintenance, confirming that changes in biosensor performance are not responsible for the increase of the K^+ signal or decline of the glucose signal.

Microdialysis was continued until the patients were moved from the intensive care unit to a rehabilitation ward, at which time all neuromonitoring stopped according to the site-specific standard of care. In three patients, glucose levels were initially normal and then declined to essentially zero: in these patients, imaging indicated that the probes were placed in the cortex but did not show clearly whether white or gray matter was involved. In a fourth patient, glucose levels were persistently low, but CT imaging was unable to confirm the placement of the probe in the parenchyma. Because of the limited number of cases thus far, we make no attempt to correlate microdialysis findings with patient outcomes (clinical microdialysis is on hold at this time due to pandemic-related restrictions). However, the similarities in the outcomes from injured animals and this small group of TBI patients motivate further investigation of the glucose decline, in particular.

Experimental Design for coMD in Rats. Studies in animals were designed to provide deeper insight into the glucose decline by means of retrodialysis and histological analyses of the probe tracks. Our objectives were to (1)

https://doi.org/10.1021/acschemneuro.1c00231
ACS Chem. Neurosci. 2021, 12, 3588−3597

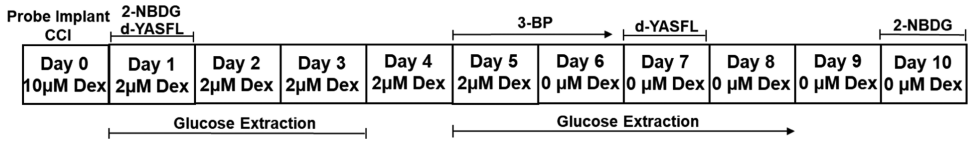

Figure 2. Time line of studies in rats. CCI and probe insertion occurred on day 0. Retrodialysis of Dex occurred on days 0−5. Retrodialysis of glucose occurred on days 1−3 (predecline) and 5−8 (postdecline); similarly, retrodialysis of d-YASFL occurred on days 1 and 7. Retrodialysis of 3-BP occurred after days 5−6 (postdecline). Retrodialysis of 2-NBDG occurred on days 1 and 10.

confirm the functionality of the glucose monitoring system and (2) investigate the mechanism driving the glucose decline after injury.

Figure 2 explains the time line of our studies. On day 0, experimental rats (n = 10) received a CCI injury and a microdialysis probe, while control rats (n = 10) received a microdialysis probe without CCI. The probes were perfused continuously for 10 days. Glucose declined to essentially zero by day 5 in some and by day 7 in all, injured rats but none of the control rats. Retrodialysis procedures were performed in subgroups of the experimental and control rats on days 1−3 and days 5−10: after CCI, days 1−3 and 5−10 are pre- and postdecline, respectively. We performed retrodialysis of the following substances: d-YASFL, a diffusion marker; glucose; 3-BP, a glycolysis inhibitor; and 2-NBDG, a fluorescently tagged analogue of 2-deoxyglucose. Each rat underwent multiple retrodialysis procedures (n values stated in the following sections) but not more than one per day: no rats received both 3-BP and 2-NBDG. After microdialysis, brain tissues were collected for histology.

Retrodialysis of d-YASFL. d-YASFL is a non-native pentapeptide used recently as an internal standard for the determination of neuropeptides in brain dialysates.[31,32] We know of only one peptidase found in the gut of a marine mollusk and able to hydrolyze a peptide containing a D-amino acid.[33] Thus, to the best of our knowledge, d-YASFL is neither a substrate for any metabolic enzymes nor a ligand for any receptors or transporters in the rat brain. We therefore hypothesize microdialysis of d-YASFL to be diffusion-controlled.

The concentration of a solute in dialysate comprises solute recovered from the external medium and solute delivered by retrodialysis but not extracted from the probe[34]

$$C_{out} = R \cdot C_{ext} + (1 - E) \cdot C_{in} \quad (1)$$

where C_{out} is the solute concentration in dialysate at the probe outlet, C_{in} is the solute concentration at the probe inlet, C_{ext} is the solute concentration in the external medium, R is the recovery fraction, and E is the extraction fraction. Rearranging eq 1 gives the equation for the plot of the concentration differences, $C_{in} - C_{out}$ vs C_{in}

$$C_{in} - C_{out} = E \cdot C_{in} - R \cdot C_{ext} \quad (2)$$

which has a slope of E and a y-intercept of $-R \cdot C_{ext}$, the negative of the solute concentration recovered in the dialysate when C_{in} is zero. Equations 1 and 2 apply to the simple case that E and $R \cdot C_{ext}$ are constants, as expected for a diffusion-controlled solute such as d-YASFL (since d-YASFL is not a brain component, $R \cdot C_{ext}$ is zero).

Figure 3 reports plots of the concentration differences for d-YASFL in injured and control animals on days 1 and 7. The E values were determined from the slopes obtained by linear regression. There were no significant differences in the E values for d-YASFL among the four experimental conditions. The

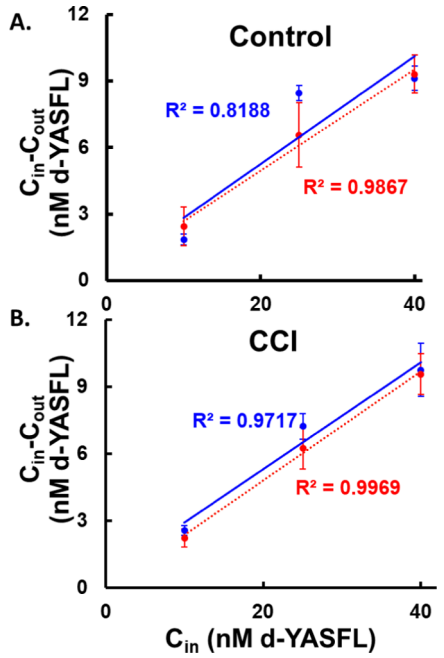

Figure 3. Concentration difference plots for d-YASFL in (A) control rats (n = 3) and (B) rats injured by CCI (n = 5) on day 1 (in blue) and day 7 (in red). Data points are means ± SEM. There were no significant differences among the slopes of the lines as determined by linear regression (ANOVA, p = 0.9872).

consistency of these E values confirms that the rate of solute diffusion between the probes and surrounding tissues holds steady over time, both with and without CCI injury. These data speak against the formation of diffusion barriers as a possible mechanism for glucose decline after injury.

Retrodialysis of Glucose. Unlike d-YASFL, glucose is a substrate for the enzymes involved in its utilization and is a ligand for glucose transporters.[35−37] Figure 4 compares plots of the concentration differences for glucose from days 1 to 3 and days 5 to 8 after CCI (i.e., pre- and postdecline). The plots are nonlinear, indicating that glucose extraction is concentration-dependent and that glucose microdialysis is thus not purely diffusion-controlled. The nonlinear character of the plots indicates that glucose microdialysis operates under the influence of active biochemical events in the tissue surrounding the probe. For this reason, eqs 1 and 2 do not fully describe the details of these glucose results. However, linear regression of the plots in the range $0 < C_{in} < 1250$ μM gives r^2 values close to unity (>0.96). So, as a purely practical matter, we take the slope of this nearly linear segment of the plots as a measure of the effective E value (E_{eff}) for glucose. There is a clear and significant increase in the E_{eff} for glucose following the glucose decline after CCI.

Consistent with the results in Figure 3, Figure 4 confirms that the microdialysis membranes and surrounding tissues

https://doi.org/10.1021/acschemneuro.1c00231
ACS Chem. Neurosci. 2021, 12, 3588−3597

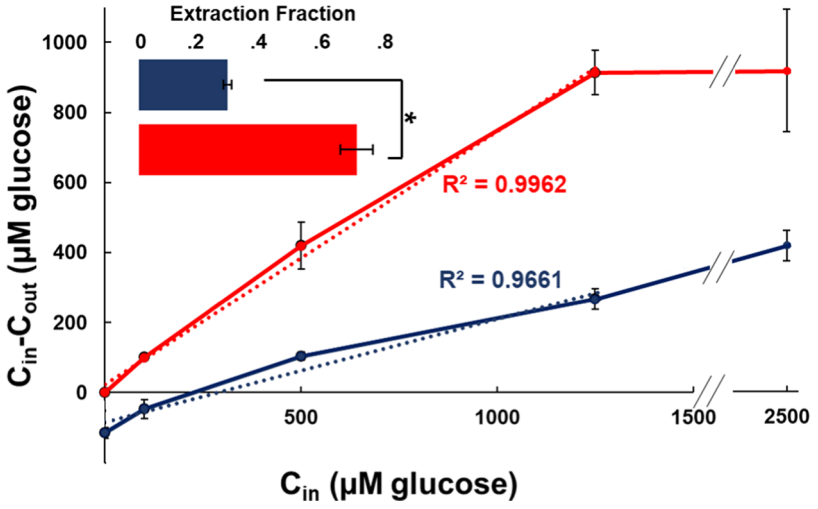

Figure 4. Concentration difference plots for glucose from rats injured by CCI (n = 5) on days 1−3 (in blue) and days 5−8 (in red). Data points are presented as mean ± SEM. The inset reports the magnitudes of the slope of the semilinear portions of the plots: for days 1−3, E_{eff} is 0.29 ± 0.01; for days 5−8, E_{eff} is 0.72 ± 0.05 (also mean ± SEM). * indicates $p < 0.05$ in a paired t-test.

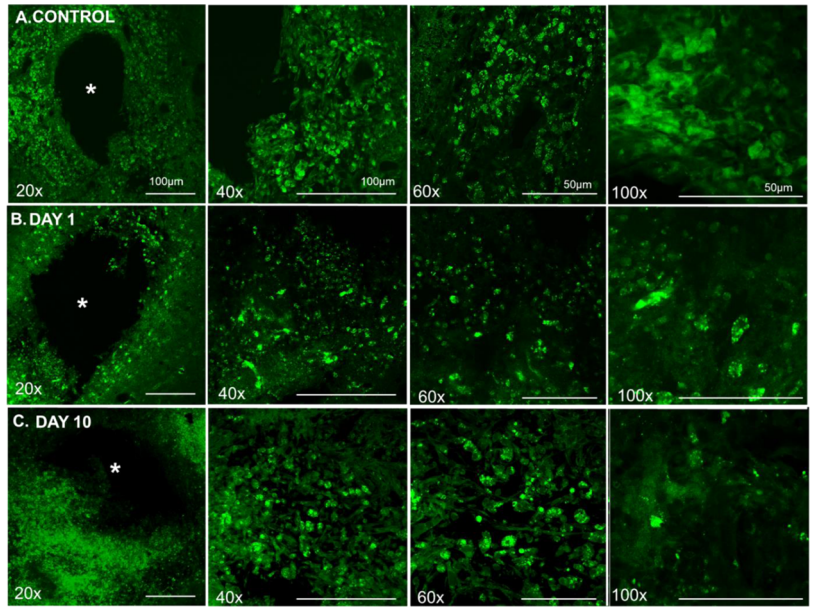

Figure 5. Representative images of intracellular fluorescence after retrodialysis of 2-NBDG in a control rat (A), on day 1 in an injured rat (B), and on day 10 in an injured rat (C). The center of each probe track is marked with an asterisk. From left to right, columns show magnifications of 20×, 40×, 60×, and 100×, with scale bars indicating 100 μm for 20× and 40× and 50 μm for 60× and 100×.

remain permeable to glucose during these experiments. A diffusion barrier would prevent glucose extraction and cause the E value to drop to zero. On the other hand, the increase in E_{eff} after following the glucose decline deserves to be explained.

The increase in the E_{eff} of glucose after injury seems to be a potentially significant finding. It implies that the tissue surrounding the probe becomes a more powerful "sink" for glucose, i.e., that the tissue increases its capacity to remove glucose from the probe. The increase in glucose removal maintains a steep concentration gradient across the dialysis membrane, thereby promoting glucose extraction. Glucose removal occurs via the blood flow and via glucose utilization by cells for the production of ATP, etc., both of which involve glucose transporters.[38] Thus, the increase in the E_{eff} of glucose signifies an increase in the rate of glucose removal by the tissue surrounding the probe.

Retrodialysis of a Fluorescent Analogue of 2-DG. We used retrodialysis of a fluorescent analogue of 2-deoxyglucose, 2-(*N*-(7-nitrobenz-2-oxa-1,3-diazol-4-yl) amino)-2-deoxyglucose (2-NBDG), to test the hypothesis that glucose extraction occurs under the influence of glucose removal via its utilization in the tissue surrounding the probe. Similar to 2-DG itself, 2-NBDG is taken up by cells via glucose transporters, undergoes phosphorylation, and accumulates inside cells.[39,40] 2-NBDG is used widely to visualize glucose utilization in astrocytes and neurons in culture and in vivo.[41−43]

Figure 5 documents the intracellular fluorescence surrounding probe tracks after retrodialysis of 2-NBDG on days 1 and 10 in control and injured rats (see Figure S2 for the quantitative assessment of these images). These images provide unequivocal evidence for the extraction of 2-NBDG from the probes into the surrounding tissue, further confirming

https://doi.org/10.1021/acschemneuro.1c00231
ACS Chem. Neurosci. 2021, 12, 3588−3597

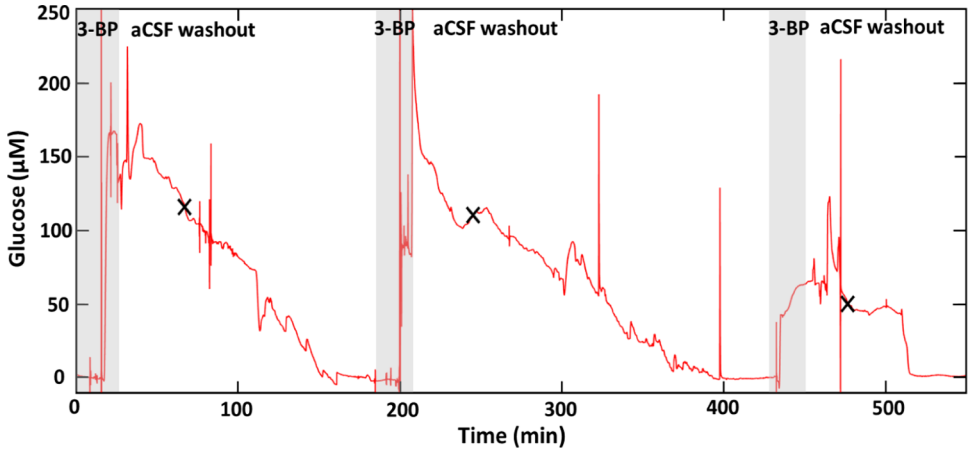

Figure 6. Representative coMD recording of glucose during three consecutive deliveries of 3-BP by retrodialysis. This recording is from a rat injured by CCI: data were collected after the postinjury glucose decline. Gray sections indicate each 30 min delivery of 3-BP: upon termination of retrodialysis, the perfusate was reset to aCSF. The "X" indicators mark the time point 30 min after the termination of 3-BP retrodialysis: the glucose concentrations at these time points were used to quantify the glucose concentration (summarized in Figure S6) to avoid the effect of 3-BP on the sensitivity of the glucose biosensors.

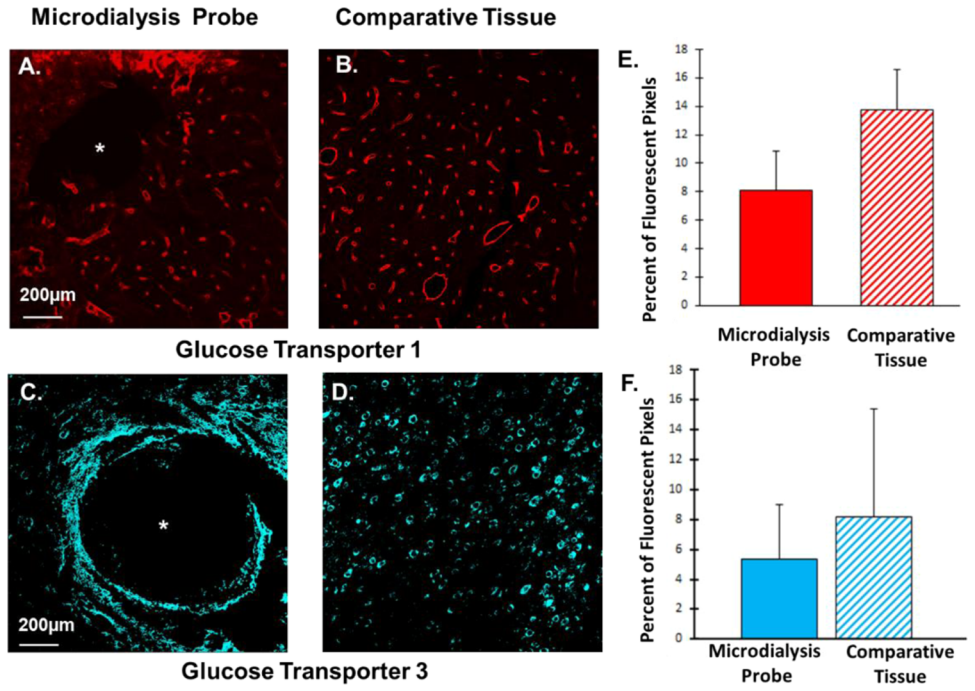

Figure 7. Immunofluorescence of glucose transporters 1 and 3 (red and blue, respectively) in the vicinity of a probe track (left) on day 10 after CCI and comparative tissues (right, B, D). The probe track is in the center of the images and marked with an asterisk (A, C). Scale bars are 200 μm. Quantitative assessment (E, F) of images of probe tracks and ipsilateral comparative tissues; error bars are SEM assessment of n = 9 images per group, as detailed in the Methods section.

their permeability, as well as 2-NBDG uptake by glucose transporters and intracellular accumulation after phosphorylation. Thus, Figure 5 confirms the ongoing glucose uptake and utilization in the vicinity of the probes over time, both with and without CCI.

Retrodialysis of a Glycolysis Inhibitor. We used retrodialysis of 3-bromopyruvate (3-BP), a well-known inhibitor of glycolysis,[44] to test the hypothesis that glucose utilization likewise affects glucose recovery. 3-BP targets hexokinase II and has been used widely to study glycolysis in cancer cells.[45−48] We performed retrodialysis of 3-BP (5 mM) for periods of 30 min in injured rats on days 5−9, >24 h after the glucose decline. Calibration studies confirm that the glucose biosensors do not detect 3-BP (Figure S3). However, 3-BP reduces the sensitivity of the biosensors (<30%): this effect is reversible, as the sensitivity returns to its pre-3-BP value by 30 min after the termination retrodialysis (Figures S4 and S5). To account for the effect of 3-BP on sensitivity, quantitative assessment of the change in glucose was performed 30 min after the termination of retrodialysis.

Retrodialysis of 3-BP increased dialysate glucose levels (Figure 6). When retrodialysis was terminated, glucose levels returned to essentially zero. As reported in Figure 6, we performed multiple 3-BP retrodialysis deliveries in some individual rats. We delivered 3-BP a total of 17 times to n = 5 CCI rats, and the dialysate glucose level increased every time

https://doi.org/10.1021/acschemneuro.1c00231
ACS Chem. Neurosci. 2021, 12, 3588−3597

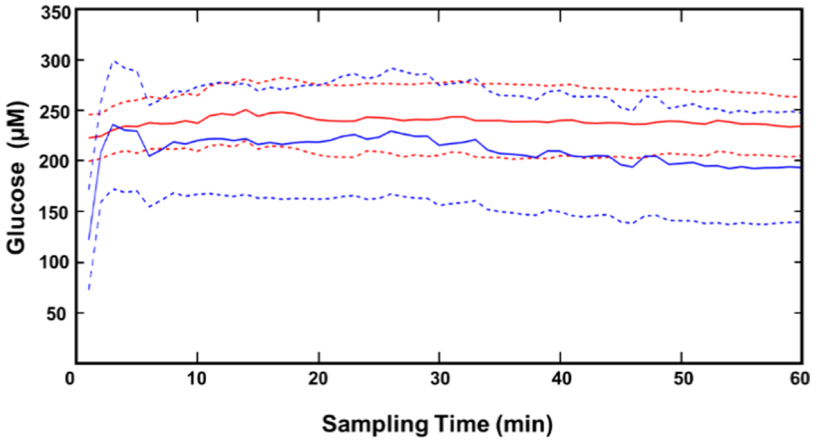

Figure 8. Recordings of glucose by coMD in control rats on day 1 (red) and day 7 (blue) (solid lines are the means, dotted lines are the ±SEMs, n = 4).

(summarized in Figure S6). These data confirm (1) that glucose recovery by microdialysis is also utilization-dependent and (2) that the probes maintain their functionality for glucose recovery after a CCI injury.

Immunofluorescence of Glucose Transporters. Figures 4−6 suggest that the microdialysis extraction and recovery of glucose occur under the influence of glucose transporters. In the brain, glucose transporters 1 and 3 are associated with blood vessels and parenchyma, respectively.[37,39,49] Immunofluorescence confirms the presence of glucose transporters 1 and 3 in the vicinity of probe tracks on day 10 after CCI (Figure 7A−D). Quantitative assessment of multiple images (n = 9 images from n = 3 rats; Figure 7E,F) found no significant differences between immunolabeling of regions of interest surrounding the probe tracks and ipsilateral comparative tissues.

Dex-Enhanced coMD of Glucose for 10 Days in Control Rats. Dialysate glucose levels fall to essentially zero by day 7 after CCI. Figure 8 confirms that this event is specific to injured animals and did not occur in rats in the noninjured control group.

CONCLUSIONS

The current study (1) establishes concordance between the outcomes of Dex-enhanced coMD after CCI in animals and TBI in patients; (2) confirms the functionality of Dex-enhanced microdialysis for monitoring intracranial glucose for 10 days after CCI injury in experimental animals; and (3) demonstrates that Dex-enhanced microdialysis extraction and recovery of glucose are coupled to glucose utilization in the tissue surrounding the probes. From this, we conclude that glucose utilization is involved in a mechanism that drives the glucose decline after CCI.

We have previously documented the functionality of long-term Dex-enhanced microdialysis. However, some of our prior studies were performed in the rat striatum and focused on monitoring dopamine.[21,23] We monitored K^+ and glucose in the rat cortex but without CCI.[24] Thus, the use of Dex-enhanced microdialysis for multiple days after CCI represents a new paradigm for intracranial monitoring. Robbins et al.[25] presented two lines of evidence for the functionality of microdialysis in rats after CCI. First, we reported the continued recovery of K^+ after the glucose decline. Second, we used mass spectrometry to show the presence of higher-molecular-weight components in dialysate samples. In retrospect, however, these data do not confirm the functionality of Dex-enhanced microdialysis specifically for glucose nor do they provide insight into the mechanism of the glucose decline after injury.

We detected no evidence of microdialysis system failure that might explain the glucose decline after injury. We consistently used newly prepared and calibrated glucose biosensors. Likewise, we consistently monitored the perfusion flow. The decline was specific to injured rats and did not occur in noninjured control rats (Figure 8). The consistency of d-YASFL's E values (Figure 3) confirms the absence of overt changes in solute diffusion rates in the membrane or surrounding tissues (no diffusion barriers). We confirmed that microdialysis membrane and surrounding tissues remain permeable to glucose (Figure 4), as well as to K^+,[25] d-YASFL, 3-BP, and 2-NBDG. The results of 3-BP retrodialysis (Figure 6) confirm the ability of the probes to recover glucose from injured tissues up to 9 days after implantation. Collectively, these findings confirm the functionality of the Dex-enhanced coMD for long-term glucose monitoring, including after injury by CCI.

We confirmed that the microdialysis extraction and recovery of glucose are coupled to glucose utilization in brain tissues. Figure 5 shows that 2-NBDG molecules diffused out of the probe and into the surrounding tissues and then entered cells via glucose transporters and accumulated after phosphorylation. Likewise, Figure 6 shows that 3-BP caused glucose to accumulate in the interstitial space and then diffuse into the probe. These processes depend on glucose transporters. Figure 7 documents the presence of glucose transporters 1 and 3 in the vicinity of the probe tracks 10 days after CCI.

Our findings show that the glucose decline following brain injury involves glucose utilization in the tissues surrounding the probe. Glucose utilization acts to lower the glucose concentration in the interstitial spaces surrounding the probe. During glucose retrodialysis (Figure 4), this maintains a steep concentration gradient between the probe and surrounding tissues, which promotes glucose extraction. However, during conventional microdialysis, this diminishes the concentration gradient that drives diffusion into the probe, which lowers glucose recovery. Thus, we attribute both the increase in glucose extraction and decrease in glucose recovery after CCI

https://doi.org/10.1021/acschemneuro.1c00231
ACS Chem. Neurosci. 2021, 12, 3588−3597

to increased glucose utilization in the tissue surrounding the probe.

Although our data establish that glucose microdialysis is coupled to glucose utilization, tissue glucose levels per se reflect the balance between utilization and vascular delivery.[50] Thus, our data show that glucose utilization increases after injury relative to glucose delivery, leaving open the possibility that ischemia or hypoglycemia may contribute to the postinjury glucose decline.[51] It is important to note, however, that just a decrease in delivery alone would not increase the glucose extraction fraction. Thus, the increase in glucose extraction fraction is a key finding that confirms the role of glucose utilization in the glucose decline.

The concordance between the outcomes of Dex-enhanced microdialysis in animals and patients appears to be a novel finding based on the absence of prior microdialysis studies of glucose in the CCI model. Microdialysis has been used in the CCI model before,[52,53] but prior studies did not concern glucose or K^+. Thus, the CCI model might be more useful than previously recognized for investigating the metabolic consequences of brain injury, especially considering that animal models afford the opportunity to apply retrodialysis and histological procedures. Results from the CCI model indicate a role of glucose utilization in the postinjury glucose decline: it is important to mention that this remains to be verified in TBI patients.

There are some notable differences between the present findings and prior clinical observations with microdialysis. Several prior studies attributed glucose declines to SD, especially to clusters of SD.[15,29,54] Our studies did not include ECoG as an independent measure of SD: instead, we relied on K^+ transients as a signature of SD. In our hands, the postinjury glucose decline occurred both with and without K^+ transients. One possible explanation for this discrepancy is that SDs occurred but were not detected because they did not involve the probe track. Alternatively, glucose declines may involve other mechanisms in addition to SD. An alternative mechanism is terminal herniation[9] although we did not encounter this here. Finally, as mentioned above, we have observed several K^+ transients indicative of SD in patients but these were not accompanied by changes in glucose levels. Glucose changes during SD have been observed by clinical coMD with surgical placement of the probes into the pericontusional space.[15,29,54] Our probes were placed in the less affected tissue via cranial bolts. Thus, probe placement appears to be an important consideration for monitoring the injured brain.

Overall, our study validates the conclusion that long-term declines in glucose levels detected by Dex-enhanced coMD are indicative of metabolic aberrations in the injured brain.

METHODS

Bedside Dex-Enhanced Clinical Microdialysis. Bedside Dex-enhanced microdialysis was conducted in patients with the approval of the Institutional Review Board of the University of Pittsburgh. Patients admitted to UPMC Presbyterian Hospital with severe TBI and who received intracranial pressure and brain tissue oxygen catheters as a standard of care were screened for participation. Inclusion criteria included ages of 18−70 years and an initial Glasgow Coma Scale score of 3−10, motor score not following commands. Written, informed proxy consent was obtained for placement of a microdialysis catheter (70 Microdialysis Bolt Catheter, M Dialysis AB, Johannesshov, Sweden) through an open port of the cranial bolt. These catheters have a polyamide membrane with a molecular weight cutoff of 20 kDa and an active sampling length of 10 mm. The catheters were primed with CNS perfusion fluid (M Dialysis AB) premixed by a hospital pharmacist with dexamethasone (10 μM) before sterile catheter insertion. The catheters were perfused at 2 μL/min with a 107 Microdialysis Pump (M Dialysis AB). Monitoring of K^+ and glucose in the dialysate stream was performed by continuous-online microdialysis (coMD), as described below.

Dex-Enhanced Microdialysis in Rats. All procedures involving animals were approved by the Institutional Animal Care and Use Committee of the University of Pittsburgh. Studies were performed in male Sprague-Dawley rats (Charles River, Raleigh, NC) weighing 250−350 g. Concentric-style microdialysis probes were constructed in-house with a 4 mm active sampling length using cellulose membranes with a 13 kDa molecular weight cutoff (Spectra/Por). The inlet and outlet lines were fused silica (75 μm ID, 150 μm OD). Prior to use, the probes were flushed with ethanol followed by sterile-filtered (Nalgene sterile filters, 0.2 μm pore size, Fisher, Pittsburgh, PA) artificial cerebrospinal fluid (aCSF; 142 mM NaCl, 1.2 mM $CaCl_2$, 2.7 mM KCl, 1.0 mM $MgCl_2$, and 2.0 mM NaH_2PO_4 (all salts from Sigma-Aldrich) adjusted to a pH of 7.4). In all procedures, including those involving retrodialysis, the probes were perfused at 1.67 μL/min with a syringe pump (Harvard Apparatus). Probes were inserted at an angle of 51° from vertical to ensure that the entire active length was within the cortex. The probes were perfused with aCSF containing 10 μM Dex for the first 24 h, 2 μM Dex for the next 96 h, and no Dex thereafter.

Controlled Cortical Impact. A controlled cortical impact (CCI) device (Leica Impact One, Leica Biosystems, Buffalo Grove, IL) was used to model a moderate-to-severe TBI.[27,28] The CCI site was accessed via a craniotomy posterior to bregma on the right hemisphere, sized to accommodate the 2.5 mm radius piston. A smaller craniotomy for probe placement was positioned 3 mm (edge to edge) anterior to the craniotomy for CCI. The positions of the craniotomies were selected to avoid the sutures of the skull and to avoid large blood vessels during probe implantation. For CCI, the exposed dura was impacted to a depth of 2.4 mm at an average velocity of 3.99 ± 0.03 m/s, with a 100 ms dwell time. The microdialysis probe was inserted after the CCI procedure. Noninjured control rats received neither a CCI nor a sham craniotomy.

Glucose Detection. To maintain consistency with our prior work, glucose extraction measurements were performed with the rapid-sampling microdialysis (rsMD) system described previously.[55] All other glucose measurements were performed with the continuous-online microdialysis (coMD) system recently developed by Boutelle and co-workers (Figure S1 presents example calibration data for both systems).[56] Briefly, needle-style microelectrodes for K^+ and glucose were interfaced to the outlet line of the microdialysis probe with a 3D-printed microelectrode holder (SomosWaterShed XC 11122). As the glucose sensors are handmade in-house, there is variability in their performance. Only those sensors meeting certain performance metrics were used in these studies. We used sensors exhibiting a linear response (r^2 > 0.99) over a concentration range of 50−1000 μM glucose and a sensitivity exceeding 0.5 pA/μM. In the case of microdialysis in animals, the fused silica outlet line was attached to the microelectrode holder with a 5 cm section of polyurethane tubing (0.18 mm ID × 0.36 mm OD: Instech Laboratories Inc.) to provide oxygen for glucose sensing. The clinical microdialysis catheters are constructed with polyurethane lines that were connected directly to the microelectrode holder.

Retrodialysis and Analysis of d-YASFL. A 1 mM stock solution of the pentapeptide, d-YASFL (each of the five amino acids in "d-YASFL" is D-stereoisomers, GL Biochem, Shanghai, China), was prepared by diluting the solid in purified water (Millipore Milli-Q Synthesis A10). The stock solution was stored frozen at −20 °C. Solutions for retrodialysis were prepared through serial dilution of the stock solution in aCSF containing 2 μM Dex (on days 1−3) to final concentrations of 100, 250, and 400 nM. These solutions were filtered using 0.2 μm PES syringe filters (Corning Inc., Corning, NY). Retrodialysis was performed in random order. Solutions were perfused through the microdialysis probe for 30 min each: after a

https://doi.org/10.1021/acschemneuro.1c00231
ACS Chem. Neurosci. 2021, 12, 3588−3597

10 min wait period, 20 min dialysate samples were collected at each d-YASFL concentration and stored at −20 °C. Then, 20 μL aliquots of the retrodialysis and dialysate solutions were individually diluted to a total volume of 200 μL with Optima LC-MS grade water (Fisher Chemical) in autosampler vials (MS Certified Autosampler Vials with 350 μL inserts, Thermo Scientific, Rockwood, TN) and placed in a refrigerated autosampler at 5 °C (Thermo Fisher Dionex UltiMate 3000, Thermo Scientific). The peptide labeling method, along with the HPLC and MS instrumental details, was as described in detail by Wilson et al., with the following minor modification. A sample desalting step was added by incorporating a precolumn (30 × 0.10 mm^2, Acquity 5 μm BEH C18, Waters, Milford, MA).

Retrodialysis of Glucose. Retrodialysis solutions with glucose concentrations of 0, 100, 500, 1250, and 2500 μM were prepared in aCSF with concentrations of Dex to match the day of the measurement (2 μM on days 1−3 and 0 μM on days 5−10). The rsMD glucose system was calibrated with each retrodialysis solution in descending order prior to each 30−60 min extraction measurement.

Retrodialysis of 2-NBDG. 2-(*N*-(7-Nitrobenz-2-oxa-1,3-diazol-4-yl)amino)-2-deoxyglucose (2-NBDG; ab146200, Abcam, Cambridge, MA) was dissolved in aCSF to a final concentration of 4 mM. Retrodialysis was performed for 4 h and followed by a washout with aCSF for an additional 4 h. Afterward, rats were anesthetized with isoflurane (5% by volume) and transcardially perfused with 200 mL of phosphate-buffered saline (PBS; 155 mM NaCl, 0.01 M, pH 7.4) followed by 160 mL of 4% paraformaldehyde. The brain and probe were removed and further fixed in 4% paraformaldehyde for 24 h at 4 °C. The tissue containing the probe track was cut to 35 μm sections in the plane perpendicular to the probe insertion. Sections were imaged with a FluoView 1000 (Olympus, Inc., Tokyo, Japan) at varying magnification.

Retrodialysis of 3-BP. 3-Bromopyruvate (3-BP) was dissolved in aCSF to a concentration of 5 mM. 3-BP was delivered by retrodialysis for 30 min.

Immunohistochemistry and Fluorescence Microscopy of Glucose Transporters. After microdialysis, rats were deeply anesthetized with isoflurane (5%) and perfused transcardially with cold PBS followed by cold 4% paraformaldehyde. Rats were decapitated, and the skull and brain were removed and soaked in cold 4% paraformaldehyde for at least 24 h. Brain tissues were sectioned to a thickness of 35 μm in the plane perpendicular to the probes using a cryostat. Tissue sections were rehydrated with 5 min washes with PBS, repeated twice, then incubated with Triton X-100 in PBS for 15 min, washed in 0.5% bovine serum albumin, and soaked in a blocking solution of 2% bovine serum albumin and 2% goat serum for 45 min. Sections were then incubated in primary antibody solution containing 5% goat serum, 0.1% Triton X-100, and antibodies for glucose transporters 1 and 3 (1:100 AbCAM) for 18 h at 4 °C. Sections were next washed with PBS (3 × 5 min) and incubated with 5% goat serum, 0.1% Triton X-100, and secondary antibodies (1:500 goat antimouse Alexa 488, Invitrogen, and 1:500 goat antirabbit Alexa 568, Invitrogen, Carlsbad, CA) for 2 h at room temperature. Sections were washed with PBS (4 × 5 min) and cover-slipped with Fluoromount-G (Southern Biotech, Birmingham, AL). Fluorescence microscopy was performed with a 20× objective (Olympus BX61, Olympus; Melville, NY) and Metamorph/Fluor 7.1 software (Universal Imaging Corporation; Molecular Devices).

Data Handling and Statistical Analysis. Data were collected on LabChart 7 and LabChart 8 (AD Instruments) and then exported and analyzed in MATLAB R2019a software. Statistical analyses were carried out with GraphPad Prism 9. We used ImageJ software[57] to analyze images stained for glucose transporters 1 and 3. Images were opened with ImageJ, and then the channels were split into monochrome colors (black and white). Threshold limits were applied to each image, which were then converted into a binary image and analyzed with the histogram function. The histogram function consisted of two numbers: the total number of black pixels (background) and the total number of white pixels (fluorescent). The white pixels were converted to the percent of fluorescent pixels and graphed in Excel.

■ ASSOCIATED CONTENT

Supporting Information

The Supporting Information is available free of charge at https://pubs.acs.org/doi/10.1021/acschemneuro.1c00231.

(1) Details regarding calibration of the rsMD and coMD systems, (2) quantitative assessment of 2-NBDG fluorescence images, (3) details on the response of the coMD system for glucose in the presence of 3-BP, and (4) a summary of the amplitude of the glucose responses to 3-BP retrodialysis (PDF)

■ AUTHOR INFORMATION

Corresponding Author

Adrian C. Michael − *Department of Chemistry, University of Pittsburgh, Pittsburgh, Pennsylvania 15260, United States;* orcid.org/0000-0001-9069-4664; Phone: +1 412-624-8560; Email: amichael@pitt.edu

Authors

Emily K. Gifford − *Department of Chemistry, University of Pittsburgh, Pittsburgh, Pennsylvania 15260, United States*

Elaine M. Robbins − *Department of Chemistry, University of Pittsburgh, Pittsburgh, Pennsylvania 15260, United States*

Andrea Jaquins-Gerstl − *Department of Chemistry, University of Pittsburgh, Pittsburgh, Pennsylvania 15260, United States*

Michael T. Rerick − *Department of Chemistry, University of Pittsburgh, Pittsburgh, Pennsylvania 15260, United States*

Enyinna L. Nwachuku − *Department of Neurological Surgery, University of Pittsburgh School of Medicine, Pittsburgh, Pennsylvania 15213, United States*

Stephen G. Weber − *Department of Chemistry, University of Pittsburgh, Pittsburgh, Pennsylvania 15260, United States;* orcid.org/0000-0002-7970-2632

Martyn G. Boutelle − *Department of Bioengineering, Imperial College London, London SW7 2AZ, United Kingdom;* orcid.org/0000-0003-1332-3442

David O. Okonkwo − *Department of Neurological Surgery, University of Pittsburgh School of Medicine, Pittsburgh, Pennsylvania 15213, United States*

Ava M. Puccio − *Department of Neurological Surgery, University of Pittsburgh School of Medicine, Pittsburgh, Pennsylvania 15213, United States*

Complete contact information is available at: https://pubs.acs.org/10.1021/acschemneuro.1c00231

Author Contributions

E.K.G. is the sole first author. E.K.G., E.M.R., and A.J.-G. collaborated on microdialysis in animals and patients. A.J.-G. performed all procedures associated with immunohistochemistry, fluorescence microscopy, and image analysis. M.T.R. and S.G.W. designed and implemented the analysis of d-YASFL. A.M.P., E.L.N., and D.O.O. supervised clinical microdialysis. M.G.B. designed and developed the rsMD and coMD analyzers. All authors participated in the design of the study, evaluation and interpretation of the results, and preparation of the manuscript.

Notes

The authors declare no competing financial interest.

■ ACKNOWLEDGMENTS

This work was funded by the National Institutes of Health (R01NS102725 and R21NS109875) and the University of

Pittsburgh Center for Biological Imaging (1S10RR028478-01). The authors thank J. Andrew Holms of the Swanson Center for Product Innovation, Swanson School of Engineering, University of Pittsburgh, for 3D printing the electrode holders used in this work.

■ ABBREVIATIONS

TBI, traumatic brain injury; CCI, controlled cortical impact; SD, spreading depolarization; Dex, dexamethasone; rsMD, rapid-sampling microdialysis; coMD, continuous-online microdialysis; d-YASFL, a non-native pentapeptide (dYdAdSdFdL); 2-DG, 2-deoxyglucose; 2-NBDG, 2-(*N*-(7-nitrobenz-2-oxa-1,3-diazol-4-yl) amino)-2-deoxyglucose; 3-BP, 3-bromopyruvate; LC, liquid chromatography; HPLC, high-performance liquid chromatography; MS, mass spectrometry; aCSF, artificial cerebrospinal fluid; PBS, phosphate-buffered saline; C_{ext}, external concentration; C_{out}, outlet concentration; C_{in}, inlet concentration and retrodialysis concentration; E, extraction fraction; E_{eff}, effective extraction fraction; R, recovery fraction

■ REFERENCES

(1) Dewan, M. C.; Rattani, A.; Gupta, S.; Baticulon, R. E.; Hung, Y.-C.; Punchak, M.; Agrawal, A.; Adeleye, A. O.; Shrime, M. G.; Rubiano, A. M.; Rosenfeld, J. V.; Park, K. B. Estimating the Global Incidence of Traumatic Brain Injury. *J. Neurosurg.* **2018**, *130*, 1−18.

(2) Liaison, O. *Hope Through Research*; National Institute of Neurological Disorders and Stroke, National Institutes of Health, 2020.

(3) Stein, S. C.; Georgoff, P.; Meghan, S.; Mizra, K.; Sonnad, S. S. 150 Years of Treating Severe Traumatic Brain Injury: A Systematic Review of Progress in Mortality. *J. Neurotrauma* **2010**, *27*, 1343−1353.

(4) Vella, M. A.; Crandall, M. L.; Patel, M. B. Acute Management of Traumatic Brain Injury. *Surg. Clin. North Am.* **2017**, *97*, 1015−1030.

(5) Hartings, J. A.; Bullock, M. R.; Okonkwo, D. O.; Murray, L. S.; Murray, G. D.; Fabricius, M.; Maas, A. I. R.; Woitzik, J.; Sakowitz, O.; Mathern, B.; Roozenbeek, B.; Lingsma, H.; Dreier, J. P.; Puccio, A. M.; Shutter, L. A.; Pahl, C.; Strong, A. J. Spreading Depolarisations and Outcome after Traumatic Brain Injury: A Prospective Observational Study. *Lancet Neurol.* **2011**, *10*, 1058−1064.

(6) Hartings, J. A.; Watanabe, T.; Bullock, M. R.; Okonkwo, D. O.; Fabricius, M.; Woitzik, J.; Dreier, J. P.; Puccio, A.; Shutter, L. A.; Pahl, C.; Strong, A. J. Spreading Depolarizations Have Prolonged Direct Current Shifts and Are Associated with Poor Outcome in Brain Trauma. *Brain* **2011**, *134*, 1529−1540.

(7) Meyerson, B. A.; Linderoth, B.; Karlsson, H.; Ungerstedt, U. Microdialysis in the Human Brain: Extracellular Measurements in the Thalamus of Parkinsonian Patients. *Life Sci.* **1990**, *46*, 301−308.

(8) Hillered, L.; Persson, L.; Ponten, U.; Ungerstedt, U. Neuro-metabolic Monitoring of the Ischaemic Human Brain Using Microdialsis. *Acta Neurochir.* **1990**, *102*, 91−97.

(9) Vespa, P. M.; McArthur, D.; O'Phelan, K.; Glenn, T.; Etchepare, M.; Kelly, D.; Bergsneider, M.; Martin, N. A.; Hovda, D. A. Persistently Low Extracellular Glucose Correlates with Poor Outcome 6 Months after Human Traumatic Brain Injury despite a Lack of Increased Lactate: A Microdialysis Study. *J. Cereb. Blood Flow Metab.* **2003**, *23*, 865−877.

(10) Hartings, J. A.; Gugliotta, M.; Gilman, C.; Strong, A. J.; Tortella, F. C.; Bullock, M. R. Repetitive Cortical Spreading Depolarizations in a Case of Severe Brain Trauma. *Neurol. Res.* **2008**, *30*, 876−882.

(11) Glenn, T. C.; Kelly, D. F.; Boscardin, W. J.; McArthur, D. L.; Vespa, P.; Oertel, M.; Hovda, D. A.; Bergsneider, M.; Hillered, L.; Martin, N. A. Energy Dysfunction as a Predictor of Outcome after Moderate or Severe Head Injury: Indices of Oxygen, Glucose, and Lactate Metabolism. *J. Cereb. Blood Flow Metab.* **2003**, *23*, 1239−1250.

(12) Hutchinson, P. J.; Jalloh, I.; Helmy, A.; Carpenter, K. L. H.; Rostami, E.; Bellander, B. M.; Boutelle, M. G.; Chen, J. W.; Claassen, J.; Dahyot-Fizelier, C.; Enblad, P.; Gallagher, C. N.; Helbok, R.; Hillered, L.; Le Roux, P. D.; Magnoni, S.; Mangat, H. S.; Menon, D. K.; Nordström, C. H.; O'Phelan, K. H.; Oddo, M.; Perez Barcena, J.; Robertson, C.; Ronne-Engström, E.; Sahuquillo, J.; Smith, M.; Stocchetti, N.; Belli, A.; Carpenter, T. A.; Coles, J. P.; Czosnyka, M.; Dizdar, N.; Goodman, J. C.; Gupta, A. K.; Nielsen, T. H.; Marklund, N.; Montcriol, A.; O'Connell, M. T.; Poca, M. A.; Sarrafzadeh, A.; Shannon, R. J.; Skjøth-Rasmussen, J.; Smielewski, P.; Stover, J. F.; Timofeev, I.; Vespa, P.; Zavala, E.; Ungerstedt, U. Consensus Statement from the 2014 International Microdialysis Forum. *Intensive Care Med.* **2015**, *41*, 1517−1528.

(13) Wright, M. J.; McArthur, D. L.; Alger, J. R.; Van Horn, J.; Irimia, A.; Filippou, M.; Glenn, T. C.; Hovda, D. A.; Vespa, P. Early Metabolic Crisis-Related Brain Atrophy and Cognition in Traumatic Brain Injury. *Brain Imaging Behav.* **2013**, *7*, 307−315.

(14) Vespa, P.; Boonyaputthikul, R.; McArthur, D. L.; Miller, C.; Etchepare, M.; Bergsneider, M.; Glenn, T.; Martin, N.; Hovda, D. Intensive Insulin Therapy Reduces Microdialysis Glucose Values without Altering Glucose Utilization or Improving the Lactate/Pyruvate Ratio after Traumatic Brain Injury. *Crit. Care Med.* **2006**, *34*, 850−856.

(15) Rogers, M. L.; Leong, C. L.; Gowers, S. A.; Samper, I. C.; Jewell, S. L.; Khan, A.; McCarthy, L.; Pahl, C.; Tolias, C. M.; Walsh, D. C.; Strong, A. J.; Boutelle, M. G. Simultaneous Monitoring of Potassium, Glucose and Lactate during Spreading Depolarization in the Injured Human Brain - Proof of Principle of a Novel Real-Time Neurochemical Analysis System, Continuous Online Microdialysis. *J. Cereb. Blood Flow Metab.* **2017**, *37*, 1883−1895.

(16) Kozai, T. D. Y.; Jaquins-Gerstl, A. S.; Vazquez, A. L.; Michael, A. C.; Cui, X. T. Brain Tissue Responses to Neural Implants Impact Signal Sensitivity and Intervention Strategies. *ACS Chem. Neurosci.* **2015**, *6*, 48−67.

(17) Jaquins-Gerstl, A.; Michael, A. C. Comparison of the Brain Penetration Injury Associated with Microdialysis and Voltammetry. *J. Neurosci. Methods* **2009**, *183*, 127−135.

(18) Nesbitt, K. M.; Jaquins-Gerstl, A.; Skoda, E. M.; Wipf, P.; Michael, A. C. Pharmacological Mitigation of Tissue Damage during Brain Microdialysis. *Anal. Chem.* **2013**, *85*, 8173−8179.

(19) Zhong, Y.; Bellamkonda, R. M. Dexamethasone-Coated Neural Probes Elicit Attenuated Inflammatory Response and Neuronal Loss Compared to Uncoated Neural Probes. *Brain Res.* **2007**, *1148*, 15−27.

(20) Abbott, N. J.; Patabendige, A. A. K.; Dolman, D. E. M.; Yusof, S. R.; Begley, D. J. Structure and Function of the Blood-Brain Barrier. *Neurobiol. Dis.* **2010**, *37*, 13−25.

(21) Varner, E. L.; Jaquins-Gerstl, A.; Michael, A. C. Enhanced Intracranial Microdialysis by Reduction of Traumatic Penetration Injury at the Probe Track. *ACS Chem. Neurosci.* **2016**, *7*, 728−736.

(22) Kozai, T. D. Y.; et al. Dexamethasone Retrodialysis Attenuates Microglial Response to Implanted Probes in Vivo. *Biomaterials* **2016**, *87*, 157−169.

(23) Jaquins-Gerstl, A.; Shu, Z.; Zhang, J.; Liu, Y.; Weber, S. G.; Michael, A. C. Effect of Dexamethasone on Gliosis, Ischemia, and Dopamine Extraction during Microdialysis Sampling in Brain Tissue. *Anal. Chem.* **2011**, *83*, 7662−7667.

(24) Varner, E. L.; Leong, C. L.; Jaquins-Gerstl, A.; Nesbitt, K. M.; Boutelle, M. G.; Michael, A. C. Enhancing Continuous Online Microdialysis Using Dexamethasone: Measurement of Dynamic Neurometabolic Changes during Spreading Depolarization. *ACS Chem. Neurosci.* **2017**, *8*, 1779−1788.

(25) Robbins, E. M.; Jaquins-Gerstl, A.; Fine, D. F.; Leong, C. L.; Dixon, C. E.; Wagner, A. K.; Boutelle, M. G.; Michael, A. C. Extended (10-Day) Real-Time Monitoring by Dexamethasone-Enhanced Microdialysis in the Injured Rat Cortex. *ACS Chem. Neurosci.* **2019**, *10*, 3521−3531.

(26) Xiong, Y.; Mahmood, A.; Chopp, M. Animal Models of Traumatic Brain Injury. *Nat. Rev. Neurosci.* **2013**, *14*, 128−142.

https://doi.org/10.1021/acschemneuro.1c00231
ACS Chem. Neurosci. 2021, 12, 3588−3597

(27) Osier, N. D.; Korpon, J. R.; Dixon, C. E. Controlled Cortical Impact Model. In *Brain Neurotrauma: Molecular, Neuropsychological, and Rehabilitation Aspects*; Kobeissy, F. H., Ed.; CRC Press/Taylor & Francis: Boca Raton, FL, 2015; Chapter 16.
(28) Dixon, C. E.; Clifton, G. L.; Lighthall, J. W.; Yaghmai, A. A.; Hayes, R. L. A Controlled Cortical Impact Model of Traumatic Brain Injury in the Rat. *J. Neurosci. Methods* **1991**, *39*, 253−262.
(29) Feuerstein, D.; Manning, A.; Hashemi, P.; Bhatia, R.; Fabricius, M.; Tolias, C.; Pahl, C.; Ervine, M.; Strong, A. J.; Boutelle, M. G. Dynamic Metabolic Response to Multiple Spreading Depolarizations in Patients with Acute Brain Injury: An Online Microdialysis Study. *J. Cereb. Blood Flow Metab.* **2010**, *30*, 1343−1355.
(30) Hashemi, P.; Bhatia, R.; Nakamura, H.; Dreier, J. P.; Graf, R.; Strong, A. J.; Boutelle, M. G. Persisting Depletion of Brain Glucose Following Cortical Spreading Depression, despite Apparent Hyperaemia: Evidence for Risk of an Adverse Effect of Leao's Spreading Depression. *J. Cereb. Blood Flow Metab.* **2009**, *29*, 166−175.
(31) Wilson, R. E.; Jaquins-Gerstl, A.; Weber, S. G. On-Column Dimethylation with Capillary Liquid Chromatography-Tandem Mass Spectrometry for Online Determination of Neuropeptides in Rat Brain Microdialysate. *Anal. Chem.* **2018**, *90*, 4561−4568.
(32) Wilson, R. E.; Jaquins-Gerstl, A.; Chen, J.; Rerick, M.; Weber, S. G. Electroosmotic Perfusion-Microdialysis Probe Created by Direct Laser Writing for Quantitative Assessment of Leucine Enkephalin Hydrolysis by Insulin-Regulated Aminopeptidase in Vivo. *Anal. Chem.* **2020**, *92*, 14558−14567.
(33) D'Aniello, A. D-Aspartic Acid: An Endogenous Amino Acid with an Important Neuroendocrine Role. *Brain Res. Rev.* **2007**, *53*, 215−234.
(34) Yang, H.; Peters, J. L.; Allen, C.; Chern, S. S.; Coalson, R. D.; Michael, A. C. A Theoretical Description of Microdialysis with Mass Transport Coupled to Chemical Events. *Anal. Chem.* **2000**, *72*, 2042−2049.
(35) Camandola, S.; Mattson, M. P. Brain Metabolism in Health, Aging, and Neurodegeneration. *EMBO J.* **2017**, *36*, 1474−1492.
(36) Dusick, J. R.; Glenn, T. C.; Lee, W. N. P.; Vespa, P. M.; Kelly, D. F.; Lee, S. M.; Hovda, D. A.; Martin, N. A. Increased Pentose Phosphate Pathway Flux after Clinical Traumatic Brain Injury: A [1,2-13C2]Glucose Labeling Study in Humans. *J. Cereb. Blood Flow Metab.* **2007**, *27*, 1593−1602.
(37) Patching, S. G. Glucose Transporters at the Blood-Brain Barrier: Function, Regulation and Gateways for Drug Delivery. *Mol. Neurobiol.* **2017**, *54*, 1046−1077.
(38) Szablewski, L. Glucose Transporters in Brain: In Health and in Alzheimer's Disease. *J. Alzheimer's Dis.* **2016**, *55*, 1307−1320.
(39) Yoshioka, K.; Takahashi, H.; Homma, T.; Saito, M.; Oh, K. B.; Nemoto, Y.; Matsuoka, H. A Novel Fluorescent Derivative of Glucose Applicable to the Assessment of Glucose Uptake Activity of *Escherichia coli*. *Biochim. Biophys. Acta* **1996**, *1289*, 5−9.
(40) Barros, L. F.; Bittner, C. X.; Loaiza, A.; Ruminot, I.; Larenas, V.; Moldenhauer, H.; Oyarzún, C.; Alvarez, M. Kinetic Validation of 6-NBDG as a Probe for the Glucose Transporter GLUT1 in Astrocytes. *J. Neurochem.* **2009**, *109*, 94−100.
(41) Loaiza, A.; Porras, O. H.; Barros, L. F. Glutamate Triggers Rapid Glucose Transport Stimulation in Astrocytes as Evidenced by Real-Time Confocal Microscopy. *J. Neurosci.* **2003**, *23*, 7337−7342.
(42) Bernardinelli, Y.; Magistretti, P. J.; Chatton, J. Y. Astrocytes Generate Na^+-Mediated Metabolic Waves. *Proc. Natl. Acad. Sci. U.S.A.* **2004**, *101*, 14937−14942.
(43) Itoh, Y.; Abe, T.; Takaoka, R.; Tanahashi, N. Fluorometric Determination of Glucose Utilization in Neurons in Vitro and in Vivo. *J. Cereb. Blood Flow Metab.* **2004**, *24*, 993−1003.
(44) Wicks, R. T.; Azadi, J.; Mangraviti, A.; Zhang, I.; Hwang, L.; Joshi, A.; Bow, H.; Hutt-Cabezas, M.; Martin, K. L.; Rudek, M. A.; Zhao, M.; Brem, H.; Tyler, B. M. Local Delivery of Cancer-Cell Glycolytic Inhibitors in High-Grade Glioma. *Neuro-Oncol.* **2015**, *17*, 70−80.
(45) Mathupala, S. P.; Ko, Y. H.; Pedersen, P. L. Hexokinase-2 Bound to Mitochondria: Cancer's Stygian Link to the "Warburg Effect" and a Pivotal Target for Effective Therapy. *Semin. Cancer Biol.* **2009**, *19*, 17−24.
(46) Pelicano, H.; Martin, D. S.; Xu, R. H.; Huang, P. Glycolysis Inhibition for Anticancer Treatment. *Oncogene* **2006**, *25*, 4633−4646.
(47) Abdel-Wahab, A. F.; Mahmoud, W.; Al-Harizy, R. M. Targeting Glucose Metabolism to Suppress Cancer Progression: Prospective of Anti-Glycolytic Cancer Therapy. *Pharmacol. Res.* **2019**, *150*, No. 104511.
(48) Vali, M.; Vossen, J. A.; Buijs, M.; Engles, J. M.; Liapi, E.; Ventura, V. P.; Khwaja, A.; Acha-Ngwodo, O.; Shanmugasundaram, G.; Syed, L.; Wahl, R. L.; Geschwind, J. F. H. Erratum: Targeting of VX2 Rabbit Liver Tumor by Selective Delivery of 3-Bromopyruvate: A Biodistribution and Survival Study (Journal of Pharmacology and Experimental Therapeutics (2008) 327 (32-37)). *J. Pharmacol. Exp. Ther.* **2015**, *353*, 560.
(49) Shah, K.; DeSilva, S.; Abbruscato, T. The Role of Glucose Transporters in Brain Disease: Diabetes and Alzheimer's Disease. *Int. J. Mol. Sci.* **2012**, *13*, 12629−12655.
(50) Vannucci, S. J.; Clark, R. R.; Koehler-Stec, E.; Li, K.; Smith, C. B.; Davies, P.; Maher, F.; Simpson, I. A. Glucose Transporter Expression in Brain: Relationship to Cerebral Glucose Utilization. *Dev. Neurosci.* **1998**, *20*, 369−379.
(51) Dreier, J. P. The Role of Spreading Depression, Spreading Depolarization and Spreading Ischemia in Neurological Disease. *Nat. Med.* **2011**, *17*, 439−447.
(52) Alessandri, B.; Heimann, A.; Filippi, R.; Kopacz, L.; Kempski, O. Moderate Controlled Cortical Contusion in Pigs: Effects on Multi-Parametric Neuromonitoring and Clinical Relevance. *J. Neurotrauma* **2003**, *20*, 1293−1305.
(53) Bell, M. J.; Kochanek, P. M.; Carcillo, J. A.; Mi, Z.; Schiding, J. K.; Wisniewski, S. R.; Clark, R. S. B.; Dixon, C. E.; Marion, D. W.; Jackson, E. Interstitial Adenosine, Inosine, and Hypoxanthine Are Increased after Experimental Traumatic Brain Injury in the Rat. *J. Neurotrauma* **1998**, *15*, 163−170.
(54) Parkin, M. C.; Hopwood, S. E.; Jones, D. A.; Hashemi, P.; Landolt, H.; Fabricius, M.; Lauritzen, M.; Boutelle, M. G.; Strong, A. J. Dynamic Changes in Brain Glucose and Lactate in Pericontusional Areas of the Human Cerebral Cortex, Monitored with Rapid Sampling on-Line Microdialysis: Relationship with Depolarisation-like Events. *J. Cereb. Blood Flow Metab.* **2005**, *25*, 402−413.
(55) Rogers, M. L.; Brennan, P. A.; Leong, C. L.; Gowers, S. A. N.; Aldridge, T.; Mellor, T. K.; Boutelle, M. G. Online Rapid Sampling Microdialysis (RsMD) Using Enzyme-Based Electroanalysis for Dynamic Detection of Ischaemia during Free Flap Reconstructive Surgery. *Anal. Bioanal. Chem.* **2013**, *405*, 3881−3888.
(56) Gowers, S. A. N.; Curto, V. F.; Seneci, C. A.; Wang, C.; Anastasova, S.; Vadgama, P.; Yang, G. Z.; Boutelle, M. G. 3D Printed Microfluidic Device with Integrated Biosensors for Online Analysis of Subcutaneous Human Microdialysate. *Anal. Chem.* **2015**, *87*, 7763−7770.
(57) Bourne, R. ImageJ. In *Fundamentals of Digital Imaging in Medicine*; Springer: London, 2010; pp 185−188.

https://doi.org/10.1021/acschemneuro.1c00231
ACS Chem. Neurosci. 2021, 12, 3588−3597